

theoretical values; the approximate values, incidentally, coincide with the exact ones.

## VI. CONCLUSION

It is shown that, first, approximate propagation constants of circular waveguide modes agree well with exact ones when the conductivity of the waveguide wall is large ( $\sigma \gg \omega \epsilon$ ) and the skin depth is smaller than the radius of the cylinder; second, that the attenuation of the  $TM_{01}$  mode is constant, i.e., independent of the material constants of the external medium and frequencies that are much lower than the cutoff frequency. The second result turns out to make the  $TM_{01}$  mode the most suitable for circular precision attenuators in the region where the attenuation of the dominant  $HE_{11}$  mode varies with frequency.

## REFERENCES

- [1] E. G. Linder, "Attenuation of electromagnetic field in pipes smaller than critical size," *Proc. Inst. Radio Eng.*, vol. 30, pp. 554-556, Dec. 1942.
- [2] A. L. Cullen, "Waveguide field pattern in evanescence modes," *Wireless Eng.*, vol. 26, pp. 317-322, Oct. 1949.
- [3] J. Brown, "Correction to the attenuation constants of piston attenuators," *Proc. Inst. Elec. Eng.*, vol. 96, pp. 491-495, pt. 3, 1949.
- [4] J. A. Stratton, *Electromagnetic Theory*. New York: McGraw-Hill, 1941, ch. 9, p. 526.
- [5] J. I. Glaser, "Attenuation and guidance of modes on hollow dielectric waveguides," *IEEE Trans. Microwave Theory Tech.*, vol. MTT-17, pp. 173-174, Mar. 1969.
- [6] Y. Yamaguchi and T. Sekiguchi, "Propagation characteristics of normal modes in hollow circular cylinder surrounded by dissipative medium," *Trans. IECE of Japan*, vol. 62-B, no. 4, pp. 368-373, Apr. 1979 (in Japanese).
- [7] V. M. Papadopoulos, "Propagation of electromagnetic waves in cylindrical waveguides and imperfectly conducting walls," *Quart. J. Mech. Appl. Math.*, vol. 7, pp. 325-334, Sept. 1954.

# Scattering of the $TE_{01}$ and $TM_{01}$ Modes on Transverse Discontinuities in a Rod Dielectric Waveguide—Application to the Dielectric Resonators

PHILIPPE GELIN, SERGE TOUTAIN, PATRICK KENNIS, AND JACQUES CITERNE

**Abstract**—Our purpose is to determine the resonance frequency together with the radiation quality factor of dielectric resonators. To do that, the reflection and the scattering properties of the  $TE_{01}$  and  $TM_{01}$  modes, incident on an abruptly ended dielectric rod, are analyzed. After the building of the complete mode spectrum on each side of the discontinuity, the continuity relations in the discontinuity plane associated with the orthogonality properties lead to a coupled integral equation system. That one is solved by means of an iterative procedure, providing all the characteristics of the discontinuity (reflection or coupling coefficients, radiation losses). Then, these solutions are used to determine the resonant frequency

and the radiation quality factor of cylindrical resonators which are considered as waveguide lengths between two interacting discontinuities.

## I. INTRODUCTION

**I**N THE LAST FEW YEARS, the availability of dielectric materials with high relative permittivity has given a great impact on the use of dielectric resonators in microwave integrated circuits (passband filters, stabilized solid-state sources).

The concept of dielectric resonator has been proposed in [1] as far back as 1939. The first analysis of the magnetic dipole resonance of cylindrical dielectric resonators of very high permittivity was treated under the assumption that all

Manuscript received October 13, 1980; revised February 3, 1981.

The authors are with the Centre Hyperfréquences et Semiconducteurs, L. A. au C. N. R. S. no. 287, Université des Sciences et Techniques de Lille, 59655 Villeneuve D'Ascq Cedex, France.

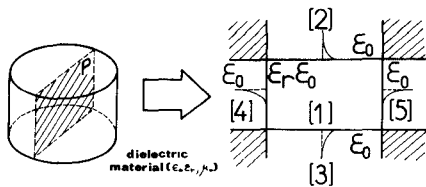


Fig. 1. The cylindrical dielectric resonator.

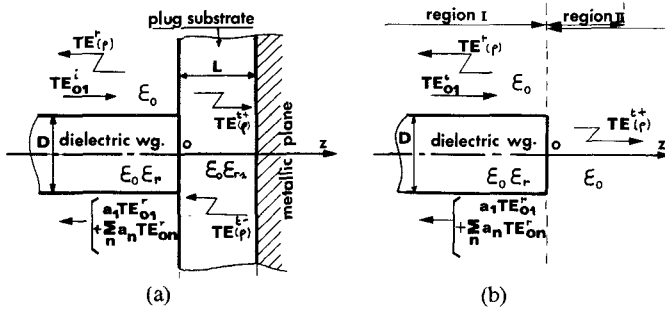


Fig. 2. (a) The substrate plugged discontinuity. (b) The abruptly ended discontinuity.

the cavity boundary surfaces are magnetic walls [2], [3]. This hypothesis did not agree with the experimental results. So the theory has been improved in [4]–[6] by considering only the extended cylindrical boundary surface as a magnetic wall, the fields decreasing from the flat surfaces outside the resonator in a restricted part of the space. A more satisfactory approach [7], [8] consists in having the field leakage through the cylindrical surface into regions 4 and 5 (see Fig. 1) and through the flat surfaces into regions 2 and 3. At this stage of the study, for the high permittivities, the calculated and experimental resonant frequencies are in very good agreement though these methods do not take into account the electromagnetic fields in the shaded areas. Nevertheless, no information on the radiation losses of this device can be expected. Only the asymptotic solution proposed by Verplanken [9], [10] allows the determination of the radiation quality factor and takes into account the field penetration in the whole space outside the resonator.

In this paper, we present a quite different and new analysis of the cylindrical resonator. This analysis proceeds in two steps. First, we study the electromagnetic behavior of an abruptly ended dielectric rod in the two cases which are presented in Fig. 2, with incident  $TE_{01}$  and  $TM_{01}$  modes. The technique which is used consists of transforming the continuity relations obtained by matching the transverse electromagnetic fields at the discontinuity interface into coupled singular integral equations. Then, these equations are solved via the conventional Neuman series solution [11]–[13]. In a second step, we take into account the interaction between such discontinuities in order to determine the resonant frequency and the radiation quality factor of dielectric resonators.

## II. DISCONTINUITY ANALYSIS

Our purpose is to derive the resonant frequencies together with the radiation  $Q$ -factors of the magnetic and electric dipole mode ( $TE_{01\delta}$ ,  $TM_{01\delta}$ ) of a cylindrical dielec-

tric resonator. The trapped waves for the “on substrate” resonator are reflected by two types of discontinuities: the abruptly ended discontinuity and the substrate plugged discontinuity [Fig. 2].

We focus our attention on the substrate plugged rod configuration, as shown in Fig. 2, which can be changed into an abruptly ended one by choosing  $L=\infty$  and  $\epsilon_{r1}=1$ . The waves are incident from the left on the discontinuity, and the problem is to find the reflection and the scattering coefficients of these incident waves. For brevity’s sake, only the  $TE_{01}$  excitation is treated in detail. The extension to the  $TM_{01}$  case presents no additional difficulty.

In the discontinuity plane  $z=0$ , we have to match the tangential electric and magnetic fields which are azimuthal (subscript  $\theta$ ) and radial (subscript  $r$ ), respectively. The continuity relations can be expressed as

$$\begin{aligned} & \left[ \begin{array}{l} E_{\theta 1}^i \\ H_{r1}^i \end{array} \right] + a_1 \left[ \begin{array}{l} E_{\theta 1}^r \\ H_{r1}^r \end{array} \right] + \sum_{n>1} a_n \left[ \begin{array}{l} E_{\theta n}^r \\ H_{r1}^r \end{array} \right] + \int_0^\infty q^r(\rho) \left[ \begin{array}{l} E_{\theta}^r(\rho) \\ H_r^r(\rho) \end{array} \right] d\rho \\ & \text{incident} \quad \text{reflected} \quad \text{reflected continuous} \\ & \nwarrow \text{guided modes} \nearrow \quad \text{modes} \\ & = \int_0^\infty q^{t+}(\rho) \left[ \begin{array}{l} E_{\theta}^{t+}(\rho) \\ H_r^{t+}(\rho) \end{array} \right] d\rho + \int_0^\infty q^{t-}(\rho) \left[ \begin{array}{l} E_{\theta}^{t-}(\rho) \\ H_r^{t-}(\rho) \end{array} \right] d\rho. \\ & \text{transmitted continuous modes} \end{aligned}$$

The fields of the left-hand side of the above equation is a superposition of the incident guided  $TE_{01}$  mode (superscript  $i$ ), of the reflected  $TE_{0n}$  guided modes ( $n>1$ ), and of the reflected continuous TE modes (superscript  $r$ ) in region I. On the right-hand side of this equation, we have a superposition of the transmitted continuous TE modes in region II (superscript  $t+$  for the modes incident towards the metallic plane, superscript  $t-$  for the others reflected on the metallic plane). The constant  $a_1$  is the reflection coefficient of the incident  $TE_{01}$  mode while the constants  $a_n$  ( $n>1$ ) are the coupling coefficients of the incident mode on the reflected and guided  $TE_{0n}$  modes in region I.

The functions  $q^r(\rho)$  are the coupling amplitudes of the backward-scattered continuous modes in region I. Backward and forward coupling amplitudes of transmitted continuous modes in region II are denoted by functions  $q^{t+}(\rho)$  and  $q^{t-}(\rho)$ , respectively. The variable  $\rho$  is both the transverse wavenumber outside the rod in region I and the transverse wavenumber inside the dielectric plug. If we denote  $\beta(\rho)$  and  $\beta_1(\rho)$  the phase constants of the continuous modes in region I and in region II, respectively, then these transverse wavenumbers can be defined as

$$\rho^2 = k_0^2 - \beta^2(\rho) \quad \text{or} \quad \rho^2 = k_0^2 \cdot \epsilon_{r1} - \beta_1^2(\rho),$$

$$\text{with } k_0 = \omega \sqrt{\epsilon_0 \mu_0}.$$

The boundary condition at the metallic plane ( $z=L$ ), provides a simple relation between functions  $q^{t+}(\rho)$  and  $q^{t-}(\rho)$ , namely

$$q^{t-}(\rho) = -q^{t+}(\rho) \cdot \exp(-2j\beta_1(\rho)L).$$

If we introduce an indicator  $\Delta$ , with  $\Delta=1$  if the metallic plane exists, and  $\Delta=0$  if the metallic plane is removed, we

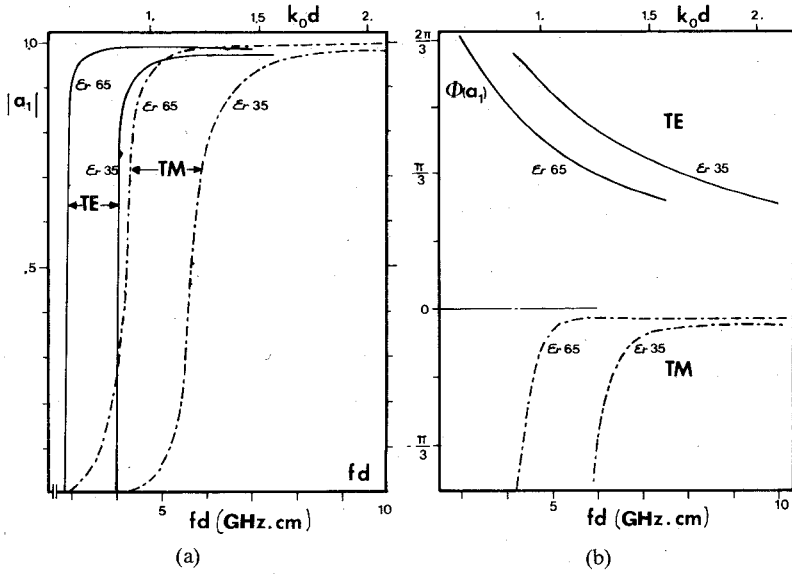


Fig. 3. (a) Moduli of the reflection coefficient  $a_1$  for the abruptly ended discontinuity. —: incident TE<sub>01</sub> mode. ---: incident TM<sub>01</sub> mode. (b) Phases of the reflection coefficient  $a_1$  for the abruptly ended discontinuity. —: incident TE<sub>01</sub> mode. ---: incident TM<sub>01</sub> mode.

can treat the abruptly ended circular dielectric waveguide together with the substrate plugged discontinuity by rewriting the above boundary condition as

$$q^{t-}(\rho) = -q^{t+}(\rho) \cdot \Delta \cdot \exp(-2j\beta_1(\rho)L).$$

Taking account of the simple relations in the two regions between the backward and forward electric and magnetic fields [see Appendix], the general mode matching equations at  $z=0$  can, consequently, be written as follows:

$$\begin{aligned} \left[ \frac{1+a_1}{\beta_1(1-a_1)} \right] E_{\theta 1}^i + \sum_{n>1} \left[ \frac{a_n}{-\beta_n a_n} \right] E_{\theta n}^i \\ + \int_0^\infty \left[ \frac{q'(\rho)}{-\beta(\rho)q'(\rho)} \right] E_\theta^i(\rho) \cdot d\rho \\ = \int_0^\infty \left[ \frac{q^{t+}(\rho) \cdot (1-X)}{\beta_1(\rho) \cdot q^{t+}(\rho) \cdot (1+X)} \right] E_\theta^i(\rho) \cdot d\rho \quad (1) \end{aligned}$$

$$\left[ \frac{a_n}{1} \right] = \frac{\pi}{2\omega\mu_0 P} \int_0^\infty q^{t+}(\rho) \left( \beta_n(1-X) \left[ \frac{-}{+} \right] \beta_1(\rho)(1+X) \right) \cdot \int_0^\infty r \cdot E_\theta^i(\beta) \cdot E_{\theta n}^i \cdot dr \cdot d\rho \quad (2)$$

where  $X = \Delta \cdot \exp(-2j\beta_1(\rho)L)$ .

We are going to use the orthogonality properties between the modes of the same region in order to derive a set of coupled integral equations between the unknown coefficients  $a_n$  ( $n > 1$ ),  $q'(\rho)$ , and  $q^{t+}(\rho)$ . We first multiply (1) and (2) by  $E'(\rho)$  and use orthogonality, then multiply again the transformed (1) by  $\beta_1$  before adding up; we obtain the following equation:

$$\begin{aligned} q^{t+}(\rho) = \frac{\pi \beta_1(\rho)}{\omega\mu_0 P} \cdot \frac{1}{(\beta_1(1-X) + \beta_1(\rho)(1+X))} \\ \cdot \left[ \sum_{n>1} a_n (\beta_1 - \beta_n) \int_0^\infty r \cdot E_{\theta n}^i \cdot E_\theta^i(\rho) \cdot dr \right. \\ \left. + \int_0^\infty q'(\rho') (\beta_1 - \beta(\rho')) \int_0^\infty r \cdot E_\theta^i(\rho') \cdot E_\theta^i(\rho') \cdot dr \cdot d\rho' \right] \\ + t(\rho) \quad (3) \end{aligned}$$

with

$$\begin{aligned} t(\rho) = \frac{\pi \beta_1(\rho)}{\omega\mu_0 P} \frac{1}{(\beta_1(1-X) + \beta_1(\rho)(1+X))} \\ \times 2\beta_1 \int_0^\infty r \cdot E_\theta^i(\rho) \cdot E_\theta^i(\rho) \cdot dr. \end{aligned}$$

The function  $t(\rho)$  does not depend on the unknown coefficients; furthermore, it has an analytical expression and represents the solution obtained by neglecting the reflected continuous and guided ( $n > 1$ ) waves. After similar operations we obtain

$$\begin{aligned} q'(\rho) = \frac{\pi \beta_1(\rho)}{\omega\mu_0 P} \frac{1}{2\beta_1(\rho)} \int_0^\infty q^{t+}(\rho) (\beta_1(\rho)(1-X) \\ - \beta_1(\rho)(1+X)) \int_0^\infty r \cdot E_\theta^i(\rho) \cdot E_\theta^i(\rho) \cdot dr \cdot d\rho \quad (4) \end{aligned}$$

$$\begin{aligned} \left[ \frac{a_n}{1} \right] = \frac{\pi}{2\omega\mu_0 P} \int_0^\infty q^{t+}(\rho) \left( \beta_n(1-X) \left[ \frac{-}{+} \right] \beta_1(\rho)(1+X) \right) \\ \cdot \int_0^\infty r \cdot E_\theta^i(\beta) \cdot E_{\theta n}^i \cdot dr \cdot d\rho \quad \begin{cases} n \geq 1 \\ n = 0 \end{cases}. \quad (5) \end{aligned}$$

Resolution of this coupled integral equation system ((3)–(5)) is then achieved by using an iterative procedure, the Neuman series solution [14] in which  $t(\rho)$  is the first-order solution for  $q'(\rho)$ . Further details on this resolution have been given in a previous paper [13].

Equation (6) and the power conservation equation (7) are tests of the validity of the method.

$$1 = \sum_{n>1} |a_n|^2 + \int_0^{k_0} |q'(\rho)|^2 d\rho + (1-\Delta) \int_0^{k_0} |q^{t+}(\rho)|^2 d\rho. \quad (7)$$

#### A. Numerical Results

1)  *Abruptly Ended Dielectric Rod ( $\epsilon_{r1} = 1$ , No Metallic Plane):* Fig. 3(a) and (b) illustrates the variations of the

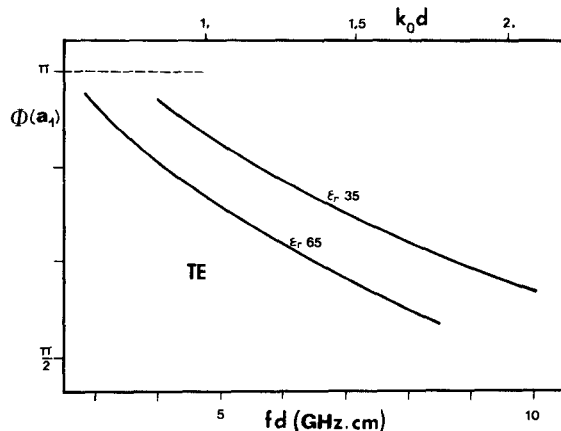


Fig. 4. Phase of the reflection coefficient  $a_1$  of the TE<sub>01</sub> mode incident in the substrate-plugged rod configuration.

TABLE I

TE <sub>01</sub> case; $\epsilon_r = 35$				TM <sub>01</sub> case; $\epsilon_r = 35$					
f.d.	Eq(5)	Eq(7)	Eq(6)	f.d.	Eq(5') *	Eq(7') *	Eq(6') *		
$a_1$	$ a_1 ^2$	$ a_1 ^2$	1	$a_1$	$ a_1 ^2$	$ a_1 ^2$	1		
4.1	-.312+j.743	.650	.655	1.001	6.	+.401-j.642	.573	.589	1.+j.001
4.2	-.317+j.806	.751	.754	1.001	6.4	+.760-j.398	.737	.741	.999
4.5	-.242+j.899	.868	.868	1.001	6.8	+.884-j.218	.830	.841	.999
5.	-.076+j.955	.918	.918	1.	7.5	+.943-j.135	.909	.913	.999
6.	+.186+j.950	.939	.939	1.001	8.5	+.963-j.115	.941	.942	1.
7.	+.368+j.896	.938	.938	1.001+j.001	10.	+.961-j.132	.941	.953	1.

\* test equations equivalent to Eqs(5), (6), (7) for the TM<sub>01</sub> case ; f.d. (GHz.cm)

moduli and of the phases of the reflection coefficient  $a_1$  of the TE<sub>01</sub> and TM<sub>01</sub> mode incident on the discontinuity (for two values of the relative permittivity:  $\epsilon_r = 35$  and  $\epsilon_r = 65$ ). We observe that the moduli increase with the permittivity for the two excitations. The modulus of the reflection coefficient of the TM excitation remains quite negligible in a large range of the normalized frequency after the cutoff. This feature corresponds to an important leakage of the energy by coupling with the radiative continuous modes. For the TE<sub>01</sub> mode, this behavior appears only at the cutoff frequency. As expected when the normalized frequency increases, the reflection coefficients  $a_1$  for the TE<sub>01</sub> as well as for the TM<sub>01</sub> excitations tend towards the limit

$$a_1 = \frac{\sqrt{\epsilon_r} - 1}{\sqrt{\epsilon_r} + 1}$$

2) *The Substrate-Plugged Rod Discontinuity:* In Fig. 4, we have plotted the evolution of the phase of the reflection coefficient  $a_1$  for the TE<sub>01</sub> excitation. In this case, as there is a perfect electric wall near the dielectric rod ( $L = 0.0635$  cm), the modulus of the reflection coefficient is quite close

to 1, whatever the normalized frequency value.

3) *Accuracy of the Method:* Accuracy of the computed results based upon (6) and (7) is illustrated by Table I. The square modulus of the reflection coefficient deduced either directly from (5) or from the power conservation integral (7) are in very good agreement. Each calculated point needs only 2 min of CPU time (4 iterations).

### III. THE DIELECTRIC RESONATOR PROBLEM

The electromagnetic parameters of the resonant mode in a cylindrical dielectric resonator can be found from the rigorous analysis of the two interacting discontinuities we have studied separately just before.

It then becomes necessary to distinguish the discontinuity parameters  $a_n$  ( $n > 1$ ),  $q'(\rho)$ , and  $q''(\rho)$  by additive superscripts I and II, depending on their type at  $z=0$  and at  $z=H$  (see Fig. 5).

For the dielectric resonator problem, the rigorous and complete equations can be expressed by writing the continuity relation between the transverse field components on both sides of the two discontinuities. As for the single discontinuity problem, the orthogonality relations change

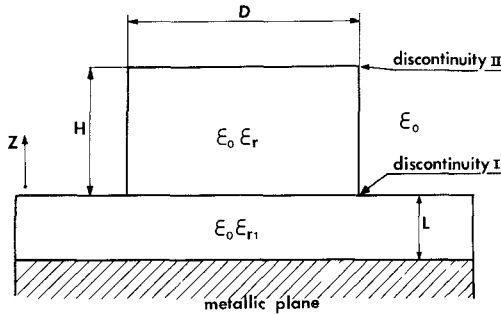
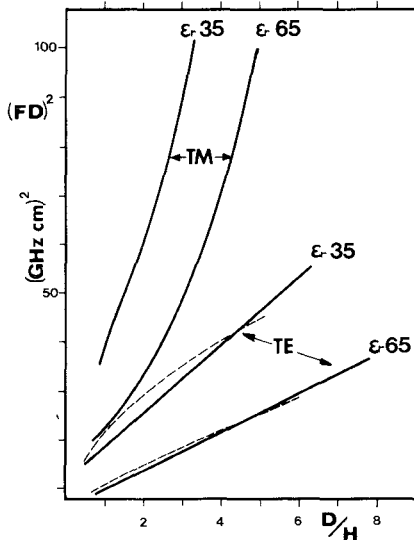


Fig. 5. The "on-substrate resonator" configuration.

Fig. 6. Resonant frequencies of the  $TE_{018}$  and  $TM_{018}$  modes for an isolated resonator. —: our results. ---: Guillon's results.

the continuity equations into a coupled integral equation set. The resonant frequency can be determined by testing the maximum of the trapped energy in the resonator and the radiation  $Q$ -factor can be obtained by the sharpness of the resonance curve versus the frequency or by the basic definition

$$Q = \omega \frac{\text{reactive energy}}{\text{average radiated power}}.$$

This rigorous formulation of the resonator problem suffers from an intrinsic weakness; it requires too long numerical calculations because the search for the resonant frequency requires, for each of trial frequencies, a complete resolution of the coupled integral system.

So, it is interesting to define a method which requires a shorter computation time. In the rigorous problem, we must consider that the incident wave on a discontinuity is a superposition of the guided resonant mode and of all the continuous modes created by the other discontinuity. But, from the previous theoretical development, it is possible to show that the power coupled by these continuous modes to the guided mode can be neglected whatever the permittivity. In this condition, we can consider that the guided mode reflected by a discontinuity results only from a coupling with the incident guided mode.

According to this remark, we can use directly the reflection coefficient obtained separately with the two types of discontinuities. The knowledge of the  $(\omega-\beta)$  diagram of the resonant mode, and of the reflection coefficient of the two discontinuities leads to use of the "transmission-line theory" to calculate the height  $H$  of the dielectric resonator to achieve a constructive phenomenon at the resonant frequency. The radiation  $Q$ -factor is derived from (8) which can be expressed as

$$Q = 2f \cdot H / [v_g \cdot (1 - |a_1^I|^2)]$$

for the isolated resonator ( $a_1^I = a_1^{II}$ ) and as

$$Q = 4f \cdot H / [v_g \cdot (2 - |a_1^I|^2 - |a_1^{II}|^2)]$$

for the resonator on substrate. In the preceding formulas,  $v_g$  denotes the group velocity of the guided mode in the dielectric rod.

#### A. Results on Cylindrical Dielectric Resonators

1) *The Isolated Resonator:* The resonant frequencies of  $TE_{018}$  and  $TM_{018}$  modes of an isolated resonator versus its  $D/H$  ratio are represented Fig. 6. Our results are in good agreement with those of Guillon [7], particularly for samples with very high permittivity. For such samples, the continuous radiated modes hardly influence the behavior

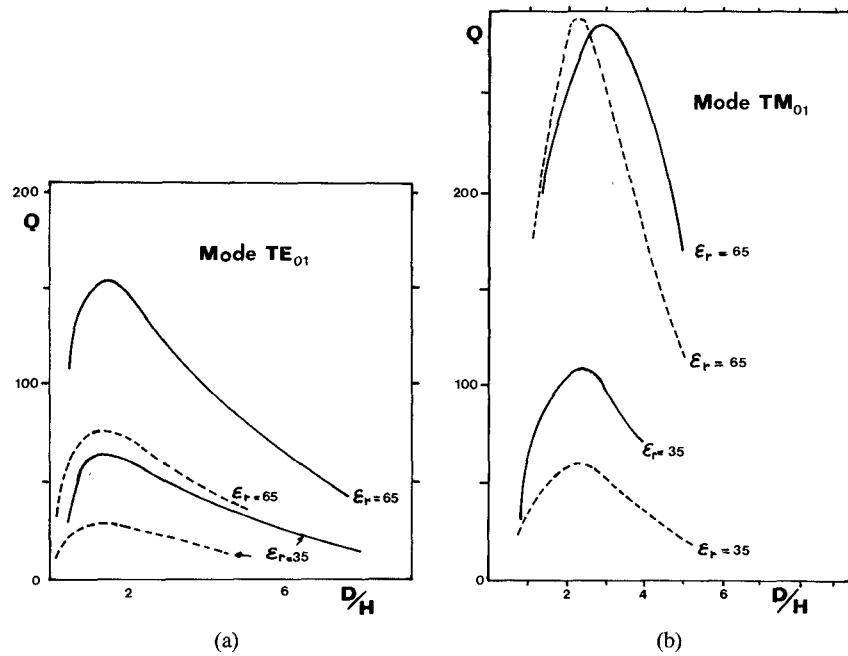


Fig. 7. Variation of the radiation  $Q$ -factor of the (a)  $TE_{018}$  and (b)  $TM_{018}$  modes for an isolated resonator. —: our results. ---: Verplanken's and Van Bladel's results.

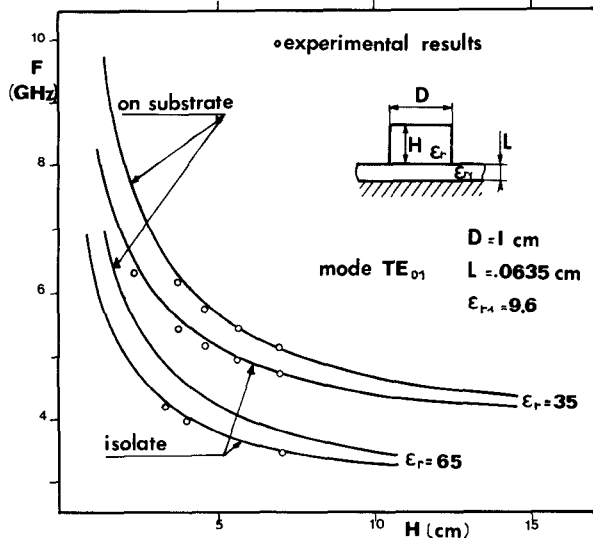


Fig. 8. Resonant frequencies of the  $TE_{018}$  mode for the isolated and "on-substrate" resonator. Comparison with the experiment. —: theoretical results. ○○○: experimental results.

of the resonator, so conventional methods of analysis fit quite well [7], [8]. In fact, the main interest of our method is to determine the radiation  $Q$ -factor of the resonator. Fig. 7(a) and (b) presents the behavior of the radiation quality factor versus the geometric parameter  $D/H$  for the two considered excitations. In these figures, the results achieved by the Verplanken approach [9], [10] have been also drawn. If the behavior of these curves is slightly identical, a quantitative agreement is only obtained for the  $TM_{01}$  excitation and for high-permittivity materials.

From the two analyses, the optimal  $D/H$  ratio is about

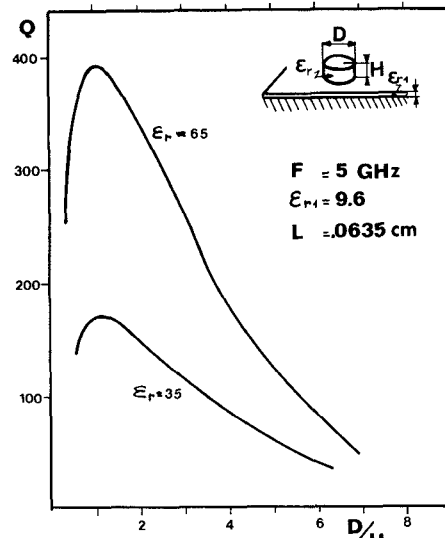


Fig. 9. Variation of the radiation  $Q$ -factor of the  $TE_{018}$  mode for an "on-substrate resonator."

1.5 for the magnetic dipolar mode and 3 for the electric dipolar mode.

2) *The resonator on substrate:* Fig. 8 shows the behavior of the resonant frequencies of the  $TE_{018}$  mode for the isolated and on-substrate resonators and for two values of permittivity ( $\epsilon_r = 35$  and  $\epsilon_r = 65$ ). Our experimental results are in good agreement with the theoretical predictions.

In Fig. 9, we present the variations of the radiation  $Q$ -factor for a resonator placed on an alumina substrate ( $\epsilon_r = 9.6$ ,  $L = 0.0635 \text{ cm}$ ) versus the quantity  $D/H$  for a

given resonant frequency  $F=5$  GHz. In this case, the optimum of the  $Q$ -factor is obtained for  $D/H$  comprised between 1 and 1.3.

#### IV. CONCLUSION

The scattering mechanism of the  $TE_{01}$  and  $TM_{01}$  modes incident in transversal dielectric rod discontinuities is analyzed by means of an integral formulation. The numerical solution is achieved by iteration via the conventional Neuman series.

This analysis allows to build a new approach for treating the resonator problem. Though we present results only for the  $TE_{01}$  and  $TM_{01}$  modes, this theory is valid for all the other excitations and can be extended to composite structures such as coaxial resonators. Moreover, it can be used whatever the permittivity and gives directly the radiation quality factor of the resonators.

#### APPENDIX

##### TRANSVERSE FIELDS OF THE GUIDED AND CONTINUOUS MODES IN THE TWO REGIONS

###### A. Guided $TE_{0n}$ Modes in Region I

The transverse fields in region I can be expressed as

$$E_{\theta n}^t = \begin{cases} A_n \mathcal{J}_1(K_n r), & r \leq a, \\ A_n \frac{\mathcal{J}_1(K_n a)}{\mathcal{K}_1(\gamma_n a)} \mathcal{K}_1(\gamma_n r), & r \geq a, \end{cases} \quad a = d/2.$$

$$H_{rn}^t = -\frac{\beta_n}{\omega \mu_0} E_{\theta n}^t, \quad \text{with } \begin{cases} K_n^2 = k_0^2 \cdot \epsilon_r - \beta_n^2 \\ \gamma_n^2 = \beta_n^2 - k_0^2 \end{cases}.$$

The characteristic equation is obtained by the continuity relation of the fields  $H_{zn}$  and  $E_{\theta n}$  at  $r=a$

$$\frac{\mathcal{J}_1(K_n a)}{\mathcal{J}_0(K_n a)} + \frac{K_n}{\gamma_n} \frac{\mathcal{K}_1(\gamma_n a)}{\mathcal{K}_0(\gamma_n a)} = 0.$$

The constant  $A_n$  is determined from the power-flow normalization

$$P = \frac{1}{2} \int_0^{2\pi} \int_0^\infty r \cdot E_{\theta n}^t \cdot H_{rn}^t \cdot dr \cdot d\theta \rightarrow A_n$$

$$= \sqrt{\frac{2\omega\mu_0 P}{\Pi a^2 \beta_n (1+K_n^2/\gamma_n^2) \cdot |\mathcal{J}_0(K_n a) \cdot \mathcal{J}_2(K_n a)|}}.$$

###### B. Continuous $TE$ Modes in Region I

In region I, the transverse fields are

$$E_{\theta}^t(\rho) = \begin{cases} B \mathcal{J}_1(\sigma r), & r \leq a \\ B \cdot [C \mathcal{J}_1(\sigma r) + D \mathcal{N}_1(\sigma r)], & r \geq a \end{cases}$$

$$H_r^t(\rho) = -\frac{\beta(\rho)}{\omega \mu_0} E_{\theta}^t(\rho), \quad \text{with } \begin{cases} \sigma^2 = k_0^2 \cdot \epsilon_r - \beta^2(\rho) \\ \rho^2 = k_0^2 - \beta^2(\rho) \\ \text{and} \\ \rho \in [0 \quad \infty[. \end{cases}$$

The continuity relation at  $r=a$  and the power-flow normal-

ization give constants  $B$ ,  $C$ , and  $D$

$$\mathcal{P} = \frac{P \cdot \beta(\rho)}{|\beta(\rho)|} = \frac{1}{2} \int_0^{2\pi} \int_0^\infty r \cdot E_{\theta}^t(\rho) \cdot H_r^t(\rho) \cdot dr \cdot d\theta$$

(see [13])

$$C = \frac{\Pi}{2} \rho a \left[ \mathcal{J}_1(\sigma a) \mathcal{N}_0(\rho a) - \frac{\sigma}{\rho} \mathcal{J}_0(\sigma a) \mathcal{N}_1(\rho a) \right]$$

$$D = -\frac{\Pi}{2} \rho a \left[ \mathcal{J}_1(\sigma a) \mathcal{J}_0(\rho a) - \frac{\sigma}{\rho} \mathcal{J}_0(\sigma a) \mathcal{J}_1(\rho a) \right]$$

$$B = \sqrt{\frac{\rho \cdot \omega \mu_0 P}{\Pi |\beta(\rho)| (C^2 + D^2)}}.$$

For the reflected mode we can write

$$E_r^t(\rho) = E^t(\rho)$$

and

$$H_r^t(\rho) = -H_r^t(\rho).$$

###### C. Continuous $TE$ Modes in Region II

The expression of the fields in region II can be written as

$$E^{t+}(\rho) = E^t(\rho) = B^t \cdot \mathcal{J}_1(\sigma r)$$

$$H^{t+}(\rho) = H^t(\rho) = -\frac{\beta_1(\rho)}{\omega \mu_0} E^t(\rho)$$

with

$$\rho^2 = k_0^2 \cdot \epsilon_r - \beta_1^2(\rho) \quad \text{and} \quad B^t = \left( \frac{\omega \mu_0 P \cdot \rho}{\Pi |\beta_1(\rho)|} \right)^{1/2}.$$

For the modes reflected by the metallic plane we can write

$$E^{t-}(\rho) = E^t(\rho) \quad \text{and} \quad H^{t-}(\rho) = -H^t(\rho).$$

#### REFERENCES

- [1] R. D. Richtmyer, "Dielectric resonators," *J. Appl. Phys.*, vol. 10, pp. 391-398, June 1939.
- [2] H. M. Schlicke, "Quasi degenerated modes in high permittivity dielectric cavities," *J. Appl. Phys.*, vol. 24, pp. 187-191, Feb. 1953.
- [3] A. Okaya, "The rutile microwave resonator," *Proc. IRE*, vol. 48, p. 1921, Nov. 1960.
- [4] Y. Yee, "An investigation of microwave dielectric resonators," *Microwave Lab. Rep. 1065*, Stanford University, Stanford, CA, July 1963.
- [5] A. Okaya and L. F. Barash, "The dielectric microwave resonator," *Proc. IRE*, vol. 50, pp. 2081-2092, Oct. 1962.
- [6] S. B. Cohn, "Microwave bandpass filters containing high-Q dielectric resonators," *IEEE Trans. Microwave Theory Tech.*, vol. MTT-16, pp. 218-227, Apr. 1968.
- [7] P. Guillon and Y. Garault, "Accurate resonant frequencies of dielectric resonators," *IEEE Trans. Microwave Theory Tech.*, vol. MTT-25, pp. 916-922, Nov. 1977.
- [8] T. Itoh and R. S. Rudokas, "New method for computing the resonant frequencies of dielectric resonators," *IEEE Trans. Microwave Theory Tech.*, vol. MTT-25, pp. 52-54, Jan. 1977.
- [9] M. Verplanken and J. Van Bladel, "The electric dipole resonances of ring resonators of very high permittivity," *IEEE Trans. Microwave Theory Tech.*, vol. MTT-24, pp. 108-112, Feb. 1976.
- [10] M. Verplanken and J. Van Bladel, "The magnetic dipole resonances of ring resonators of very high permittivity," *IEEE Trans. Microwave Theory Tech.*, vol. MTT-27, pp. 328-334, Apr. 1979.
- [11] P. Gelin, M. Petenzi, and J. Citerne, "New rigorous analysis of the step discontinuity in a slab dielectric waveguide," *Electron. Lett.*,

vol. 15, no. 12, pp. 355-356, June 1979.

[12] P. Gelin, M. Petenzi, P. Kennis, and J. Citerne, "Analysis of the scattering mechanism in an abruptly ended rod dielectric waveguide. Application to the determination of the characteristics of dielectric resonators, presented at the MTT Symposium 1980, Washington, DC.

[13] P. Gelin, M. Petenzi, and J. Citerne, "Rigorous analysis of the scattering of surface waves in an abruptly ended slab dielectric waveguide," *IEEE Trans. Microwave Theory Tech.*, vol. MTT-29, pp. 107-114, Feb. 1981.

[14] C. T. H. Baker, *The Numerical Treatment of Integral Equations*. Oxford, England: Clarendon, 1977.

# Analysis and Sensitivity Evaluation of 2 $p$ -Port Cascaded Networks

JOHN W. BANDLER, FELLOW, IEEE, AND MOHAMED R. M. RIZK, MEMBER, IEEE

**Abstract**—An exact analysis approach for efficiently evaluating the response and its sensitivities with respect to all design parameters for cascaded 2  $p$ -port networks is presented for any value of  $p$ . It is illustrated via a quasi-optical bandpass filter.

## I. INTRODUCTION

**A** GENERALIZATION of an analysis approach for 2-port cascaded networks [1] to handle 2  $p$ -port networks is presented. The generalized approach has the same advantages as those for 2-port networks. These advantages include efficient and fast analytical and numerical investigations of response, first-order sensitivities of the response with respect to variable parameters, and large-change sensitivities. The need for this generalization evolved from the fact that many microwave networks are represented as a cascade of 2  $p$ -port elements.

Thevenin and Norton equivalents for these cascaded networks can be obtained systematically using this approach. These in turn are very useful for worst case analysis [2]. As an example, a quasi-optical bandpass filter has been analyzed using this approach and the exact sensitivities

Manuscript received October 28, 1980; revised January 5, 1981. This work was supported by the Natural Sciences and Engineering Research Council of Canada under Grant A7239 and by McMaster University under a Grant from the Science and Engineering Research Board. This paper was presented at the 1980 IEEE-MTT International Microwave Symposium, Washington, DC.

The authors are with the Group on Simulation, Optimization, and Control and the Department of Electrical and Computer Engineering, McMaster University, Hamilton, Ont., Canada L8S 4L7.

of the response with respect to a parameter appearing in two of the 2  $p$ -port elements, representing the filter elements, have been evaluated.

## II. THEORY

The analysis approach consists of two principal types. The first, which we call the forward analysis, consists of initializing a  $\bar{U}^T$  matrix as  $\bar{E}_1^T$  or  $\bar{E}_2^T$ , which are defined as

$$\bar{E}_1 \triangleq \begin{bmatrix} \mathbf{1}_p \\ \mathbf{0}_p \end{bmatrix} \quad \bar{E}_2 \triangleq \begin{bmatrix} \mathbf{0}_p \\ \mathbf{1}_p \end{bmatrix}$$

where  $\mathbf{1}_p$  is the unit matrix of order  $p$ ,  $\mathbf{0}_p$  is the null matrix of order  $p$ , and successively premultiplying each constant chain matrix by the resulting matrix until an element of interest (which contains a variable parameter), a reference plane, or a termination is reached. The second type of analysis is the reverse analysis which consists of initializing a  $V$  matrix as either  $E_1$  or  $E_2$  and successively postmultiplying each constant matrix by the resulting matrix until an element of interest, a reference plane, or a termination is reached.

Consider the 2  $p$ -port element shown in Fig. 1, possessing  $p$  input ports and  $p$  output ports. Its transmission matrix is given by

$$A \triangleq \begin{bmatrix} A_{11} & A_{12} \\ A_{21} & A_{22} \end{bmatrix}$$

where  $A_{11}$ ,  $A_{12}$ ,  $A_{21}$ , and  $A_{22}$  are  $p \times p$  matrices. The input